Epigenetic Library Screen Identifies Abexinostat as Novel Regulator of Adipocytic and Osteoblastic Differentiation of Human Skeletal (Mesenchymal) Stem Cells

Ali, D.; Hamam, R.; Alfayez, M.; Kassem, Moustapha; Aldahmash, Abdullah M.; Alajez, Nehad M

Published in:
Stem Cells Translational Medicine

DOI:
10.5966/sctm.2015-0331

Publication date:
2016

Document version
Publisher's PDF, also known as Version of record

STEM CELLS TRANSLATIONAL MEDICINE®

CELL-BASED DRUG DEVELOPMENT, SCREENING, AND TOXICOLOGY

Epigenetic Library Screen Identifies Abexinostat as Novel Regulator of Adipocytic and Osteoblastic Differentiation of Human Skeletal (Mesenchymal) Stem Cells

DALIA ALI,[a] RIMI HAMAM,[a] MUSAED ALFAYEZ,[a] MOUSTAPHA KASSEM,[a,b] ABDULLAH ALDAHMASH,[a,c] NEHAD M. ALAJEZ[a]

Key Words. Epigenetic • Adipocyte • Osteoblast • Mesenchymal stem cells • Histone deacetylase inhibitors

[a]Stem Cell Unit, Department of Anatomy, College of Medicine, and [c]Prince Naif Health Research Center, King Saud University, Riyadh, Kingdom of Saudi Arabia; [b]Molecular Endocrinology and Stem Cell Research Unit, Department of Endocrinology, University of Southern Denmark, Odense, Denmark

Correspondence: Nehad M. Alajez, Ph.D., Stem Cell Unit, Department of Anatomy, College of Medicine, King Saud University, P.O. Box 305713, Riyadh 11461, Kingdom of Saudi Arabia. Telephone: 966 114679216; E-Mail: nalajez@ksu.edu.sa

Received November 5, 2015; accepted for publication March 10, 2016; published Online First on May 18, 2016.

1066-5099/2016/$20.00/0

http://dx.doi.org/10.5966/sctm.2015-0331

ABSTRACT

The epigenetic mechanisms promoting lineage-specific commitment of human skeletal (mesenchymal or stromal) stem cells (hMSCs) into adipocytes or osteoblasts are still not fully understood. Herein, we performed an epigenetic library functional screen and identified several novel compounds, including abexinostat, which promoted adipocytic and osteoblastic differentiation of hMSCs. Using gene expression microarrays, chromatin immunoprecipitation for H3K9Ac combined with high-throughput DNA sequencing (ChIP-seq), and bioinformatics, we identified several key genes involved in regulating stem cell proliferation and differentiation that were targeted by abexinostat. Concordantly, ChIP-quantitative polymerase chain reaction revealed marked increase in H3K9Ac epigenetic mark on the promoter region of *AdipoQ, FABP4, PPARγ, KLF15, CEBPA, SP7,* and *ALPL* in abexinostat-treated hMSCs. Pharmacological inhibition of focal adhesion kinase (PF-573228) or insulin-like growth factor-1R/insulin receptor (NVP-AEW51) signaling exhibited significant inhibition of abexinostat-mediated adipocytic differentiation, whereas inhibition of WNT (XAV939) or transforming growth factor-β (SB505124) signaling abrogated abexinostat-mediated osteogenic differentiation of hMSCs. Our findings provide insight into the understanding of the relationship between the epigenetic effect of histone deacetylase inhibitors, transcription factors, and differentiation pathways governing adipocyte and osteoblast differentiation. Manipulating such pathways allows a novel use for epigenetic compounds in hMSC-based therapies and tissue engineering. STEM CELLS TRANSLATIONAL MEDICINE *2016;5:1036–1047*

SIGNIFICANCE

This unbiased epigenetic library functional screen identified several novel compounds, including abexinostat, that promoted adipocytic and osteoblastic differentiation of human skeletal (mesenchymal or stromal) stem cells (hMSCs). These data provide new insight into the understanding of the relationship between the epigenetic effect of histone deacetylase inhibitors, transcription factors, and differentiation pathways controlling adipocyte and osteoblast differentiation of hMSCs. Manipulating such pathways allows a novel use for epigenetic compounds in hMSC-based therapies for tissue engineering, bone disease, obesity, and metabolic-disorders.

INTRODUCTION

Human skeletal stem cells (also known as stromal or mesenchymal stem cells) (hMSCs) are adult multipotent stem cells that have the potential to differentiate into distinct mesodermal lineage cells, such as adipocytes, osteoblasts, chondrocytes, and myocytes [1].

Lineage-specific differentiation of MSCs is determined by integrating microenvironmental cues with intracellular signaling pathways, transcriptional regulatory networks, and chromatin remodeling [2]. Nevertheless, it has been reported in several studies that epigenetic modulations could affect key transcriptional factors shaping gene expression and differentiation potentials of embryonic stem cells [3]. The modulation of chromatin structure through histone modifications includes acetylation, methylation and phosphorylation, and this modulation is referred to collectively as epigenetic regulation [4].

Epigenetic modulation refers to modulation of heritable changes in gene expression via mechanisms other than alteration of the DNA

sequence [5]. Histone acetylation is regulated by a balance of the enzymatic activity of histone acetyltransferase and histone deacetylase (HDAC) [6]. The two opposing enzymatic activities of histone acetylation and deacetylation are important for the activation of transcription [7] and regulation of gene expression in eukaryotes [8]. HDACs regulate cell differentiation and modulate tissue-specific gene expressions, as has been demonstrated in the development of neuron precursors in animal studies [9] and in clinical trials as antiproliferative and proapoptotic therapy against cancer [10, 11].

Several studies investigated the importance of chemical compound inhibitors of HDACs for their possible therapeutic effects. Inhibitors of HDACs (HDACi) induce hyperacetylation of histones, followed by the activation of specific genes through relaxation of the DNA conformation. Some HDACi have been tested for their anticancer effects in different human malignancies [12, 13]. In addition, several studies investigated the effect of HDACi on stem cell differentiation. HDACi enhanced osteoblast differentiation of human dental pulp stem cells [14] and bone marrow MSCs [10]. Dudakovic et al. [15] reported that HDACi promoted late stages of osteoblast differentiation via increasing histone H4 acetylation and regulating insulin signaling pathway in murine MC3T3. Moreover, the observed promoting effects of HDACi on osteoblast differentiation have been attributed to their regulatory effects on runt-related-transcription factor 2, a key transcription factor in osteoblast commitment [16–18]. Few studies examined the changes in HDAC during adipocyte differentiation of extramedullary fat [19–21]. Little is known about the effects of HDAC and HDACi on bone marrow adipocyte differentiation and functions.

Herein we tested the effects of several chemical compounds with effects on epigenetic state regulators and identified novel compounds with significant effects on adipocyte and osteoblast differentiation of hMSCs. One of these, abexinostat, was chosen for follow-up studies. Using chromatin immunoprecipitation combined with high-throughput DNA sequencing (ChIP-seq) technology and ChIP quantitative polymerase chain reaction (qPCR), we identified several key genes involved in regulating MSC proliferation and differentiation as putative targets for abexinostat.

Materials and Methods

Epigenetic Library

An epigenetic library, purchased from Selleckchem Inc. (Houston, TX, http://www.selleckchem.com), consisting of 24 active compounds (Table 1), was tested in the current study. Initial screen was conducted using 20, 100, and 500 nM.

Cell Culture

We used a telomerized hMSC line (hMSC-TERT) as a model for bone marrow-derived MSCs. The hMSC-TERT line was created through overexpression of the human telomerase reverse transcriptase gene (*hTERT*) [22]. hMSC-TERT expresses all known markers of primary hMSCs [22] and exhibits "stemness" characteristics by being able to form bone and bone marrow microenvironment when implanted subcutaneously in vivo [22]. For the sake of brevity, we refer to these cells as hMSCs in the rest of this article.

Cells were cultured in basal culture medium of DMEM (supplemented with 4,500 mg/l D-glucose, 4 mM L-glutamine, and 110 mg/l 10% sodium pyruvate, 10% fetal bovine serum [FBS], 1% penicillin-streptomycin, and 1% nonessential amino acids). All reagents were purchased from Thermo Fisher Scientific Life Sciences, Waltham, MA (http://www.thermofisher.com). Cells were incubated in 5% CO_2 incubators at 37°C and 95% humidity. MSC-TERT cells were cultured to reach 80%–90% confluence before addition of the compounds. The compounds were added at concentrations of 20, 100, or 500 nM for 24 hours. Afterward, the cells were exposed to adipogenic or osteoblastic induction. Control cells were treated with basal medium containing dimethyl sulfoxide (DMSO) as vehicle.

Table 1. Characteristics of the 24 compounds used in the epigenetic library screen

No.	Name of compound	Target
1	Quisinostat	HDAC1, HDAC2, HDAC4, HDAC10, HDAC11
2	Givinostat	HD2, HD1B and HD1A
3	Panobinostat	HDAC, HDAC
4	Trichostatin A	HDAC
5	Vorinostat	HDAC
6	Obatoclax mesylate	Bcl-2
7	Belinostat	HDAC
8	Abexinostat	HDAC1, HDAC2, HDAC3, HDAC6, HDAC8, DAC10
9	Dacinostat	HDAC
10	Mocetinostat	HDAC1, HDAC2, HDAC3
11	CUDC-907	PI3Kα, HDAC1, HDAC2, HDAC3, HDAC10
12	M344	HDAC
13	Tacedinaline	HDAC1
14	SRT1720	SIRT1
15	CUDC-101	HDAC, EGFR, HER2
16	Droxinostat	HDAC3, HDAC6, HDAC8
17	MC1568	HDAC1A, HDAC1B
18	Pracinostat	HDAC1, HDAC3, HDAC4, HDAC5, HDAC9, DAC10
19	Selisistat	SIRT1
20	AR-42	HDAC
21	Sodium valproate	HDAC, Autophagy & GABA receptor
22	PCI-34051	HDAC1, HDAC2, HDAC3, HDAC6, HDAC8, HDAC10
23	Romidepsin	HDAC1, HDAC2
24	Sirtinol	SIRT1, SIRT2

Adipogenic Differentiation

The adipogenic induction medium (AIM) consisted of DMEM supplemented with 10% FBS, 10% horse serum (Sigma-Aldrich, St. Louis, MO, http://www.sigmaaldrich.com), 1% penicillin-streptomycin , 100 nM dexamethasone, 0.45 mM isobutyl methyl xanthine (Sigma-Aldrich), 3 μg/ml insulin (Sigma-Aldrich), and 1 μM rosiglitazone (BRL49653). The AIM was replaced every 3 days. Cells were assessed for adipogenic differentiation on day 7. In addition, cell pellets were collected for total RNA isolation and quantification using quantitative real-time (RT) PCR of mRNA expression.

Oil Red O Staining

Adipogenic differentiation was determined by qualitative Oil Red O staining for lipid-filled mature adipocytes. Cells were washed with phosphate-buffered saline (PBS), fixed with 4% paraformaldehyde for 10 minutes, and then incubated with freshly made and filtered (0.45 μM) Oil Red O staining solution (0.05 g in 60% isopropanol; Sigma-Aldrich) for 1 hour at room temperature. Images were acquired using an inverted Zeiss microscope (Thornwood, NY, http://www.zeiss.com).

Nile Red Staining

Nile red fluorescence quantification of adipogenesis was performed using stock solution of Nile red (1 mg/ml) in DMSO that was stored at −20°C protected from light. Staining was performed on unfixed cells. Cultured differentiated cells were grown in polystyrene flat-bottom 96-well tissue culture (TC)-treated black microplates (Corning Inc., Corning, NY, http://www.corning.com) and washed once with PBS. The dye was then added directly to the cells (5 μg/ml in PBS), and the preparation was incubated for 10 minutes at room temperature, then washed twice with PBS. Fluorescent signal was measured using a SpectraMax/M5 fluorescence spectrophotometer plate reader (Molecular Devices Co., Sunnyvale, CA, https://www.moleculardevices.com) using the bottom well-scan mode, during which nine readings were taken per well using excitation (485 nm) and emission (572 nm) spectra. Furthermore, fluorescence images were taken using a FLoid cell imaging station (Thermo Fisher Scientific Life Sciences).

Osteogenic Differentiation

hMSCs were cultured as noted in the previous section and exposed to osteogenic induction medium (DMEM containing 10% FBS, 1% penicillin-streptomycin, 50 μg/ml L-ascorbic acid (Wako Chemicals GmbH, Neuss, Germany, http://www.wako-chemicals.de/), 10 mM β-glycerophosphate (Sigma-Aldrich), 10 nM calcitriol (1α,25-dihydroxyvitamin D3; Sigma-Aldrich), and 10 nM dexamethasone (Sigma-Aldrich).

Alkaline Phosphatase Activity Quantification

To quantify alkaline phosphatase (ALP) activity in control and osteoblast-differentiated hMSCs, we used the BioVision ALP activity colorimetric assay kit (BioVision, Inc., Milpitas, CA, http://www.biovision.com/) with some modifications. Cells were cultured in 96-well plates under normal or osteogenic induction conditions. On day 10, wells were rinsed once with PBS and were fixed using 3.7% formaldehyde in 90% ethanol for 30 seconds at room temperature; fixative was removed and 50 μl of *p*-nitrophenyl phosphate solution was added to each well and incubated for 20–30 minutes in the dark at room temperature until a clear yellow color developed. Reaction was subsequently stopped by adding 20 μl of stop solution. Optical density was then measured at 405 nm using a SpectraMax/M5 fluorescence spectrophotometer plate reader.

Inhibition of Focal Adhesion Kinase and Insulin-Like Growth Factor-1R/Insulin Receptor Signaling During Adipocytic Differentiation

hMSCs were cultured in Corning polystyrene flat-bottom 96-well TC-treated black microplates; after exposure to abexinostat or vehicle control for 24 hours, normal culture medium was replaced with adipogenic induction medium supplemented with focal adhesion kinase (FAK) (PF-573228) at 5 μM (Selleckchem Inc.) or insulin-like growth factor (IGF)-1R/insulin receptor (InsR) signaling inhibitor (NVP-AEW51) at 5 μM (Selleckchem Inc.). Adipogenic medium supplemented with inhibitors was replaced every 2 days. Nile red fluorescence quantification of adipogenesis was performed on day 7 as described earlier in the text.

Inhibition of WNT and Transforming Growth Factor β Signaling During Osteogenic Differentiation

hMSCs were cultured in 96-well plates; after exposure to abexinostat or vehicle control for 24 hours, normal culture medium was replaced with osteogenic induction medium supplemented with WNT (XAV939) at 1 μM (Sigma-Aldrich) or transforming growth factor β (TGFβ signaling inhibitor (SB505124) at 1 μM (Sigma-Aldrich). Osteogenic medium supplemented with inhibitors was replaced every 2 days. On day 10, ALP activity was measured as indicated above.

RNA Extraction and cDNA Synthesis

Total RNA that was isolated from cell pellets after 7 days of adipogenic differentiation and 9 days after osteogenic differentiation using the Total RNA Purification Kit (Norgen Biotek Corp., Thorold, ON, Canada, https://norgenbiotek.com/) according to the manufacturer's protocol. The concentrations of total RNA were measured using NanoDrop 2000 (ThermoFisher Scientific Life Sciences). cDNA was synthesized using 500 ng of total RNA and the ThermoFisher Scientific Life Sciences High Capacity cDNA Transcription Kit according to manufacturer's protocol.

qRT-PCR

Expression levels of adipogenic-related genes (*FABP4* and *AdipoQ*) and validation of selected upregulated genes in the microarray data were quantified using the Fast SYBR Green Master Mix and the ViiA 7 Real-Time PCR device (ThermoFisher Scientific Life Sciences). Primers used for gene expression analysis and validation are listed in supplemental online Table 4. For osteoblast-related gene expression, custom Taqman Low Density Array Cards were used (ThermoFisher Scientific Life Sciences). The assay ID for primer sets used for the osteoblast gene panel is provided in supplemental online Table 5. The 2ΔCT value method was used to calculate relative expression, and analysis was performed as previously described [23].

HDAC Enzymatic Activity Assay

HDAC enzymatic activity in control or treated hMSC-TERT cells was measured using HDAC-Glo I/II assay and screening system (Promega Inc., Madison, WI, http://www.promega.com/) according to manufacturer's protocol. Briefly, 10,000 cells, volume of 50 μl, were seeded per well in a white-walled 96-well plate and incubated with the inhibitor mixture at 37°C for 30 minutes. Trichostatin A was used as a positive control (supplied with the kit). HDAC-Glo I/II reagent (containing the substrate and the developer reagent) was added, and the solution was incubated at room temperature for 45 minutes. Luminescence was measured using a SpectraMax/M5 fluorescence spectrophotometer plate reader.

Gene Expression Profiling by Microarray

Total RNA of the samples was extracted using a Total RNA Purification Kit (Norgen Biotek Corp.) according to the manufacturer's instructions. One hundred fifty nanograms of total RNA was labeled using a low input Quick Amp Labeling Kit (Agilent Technologies, Santa Clara, CA, http://www.agilent.com) and then hybridized to the Agilent Human SurePrint G3 Human GE 8 $\times$ 60k microarray chip. All microarray experiments were performed at the Microarray Core Facility (Stem Cell Unit, Department of Anatomy, King Saud University College of Medicine, Riyadh, Saudi Arabia). The extracted data were normalized and analyzed using GeneSpring 13.0 software (Agilent Technologies). Pathway analyses were performed using the single experiment pathway analysis feature in GeneSpring 13.0 as described earlier. Two-fold cutoff and $p < .05$ (Benjamini-Hochberg multiple testing corrected) were used to determine significantly changed transcripts.

Immunoblotting

Total cellular protein was extracted with radioimmunoprecipitation assay lysis solution (Norgen Biotek Corp.). Ten micrograms of the protein were resolved by Mini-PROTRANTGX Stain Free precast gels and transferred to a polyvinylidene fluoride (PVDF) membrane by Trans-Blot Turbo Mini PVDF Transfer Pack (Bio-Rad Laboratories, Hercules, CA, http://www.bio-rad.com/). Blots were incubated with primary antibodies overnight at 4°C in Tris-buffered saline-Tween (0.05%) with 5% nonfat milk at the designated dilution against acetyl-histone H3 (Lys9) (C5B11) rabbit monoclonal antibody (mAb) (1:1,000; catalog no. 9649, Cell Signaling Technology, Danvers, MA, http://www.cellsignal.com), acetyl-histone H4 (Lys8) antibody (1:1,000; catalog no. 2594, Cell Signaling Technology), and di-methyl-histone H3 (Lys4) (C64G9) rabbit mAb (1:1,000; catalog no. 9725, Cell Signaling Technology). The membrane was subsequently incubated with anti-rabbit IgG-horseradish peroxidase (HRP)-linked antibody (1:3,000; catalog no. 7074p2, Cell Signaling Technology). Membranes were probed with HRP-conjugated anti-glyceraldehyde-3-phosphate dehydrogenase (GAPDH) antibody (1:10,000, ab9482; Abcam, Cambridge, MA, http://www.abcam.com/) as loading control. Imaging was conducted using the ChemiDoc MP imager (Bio-Rad Laboratories). Band intensity was quantified using the band quantification tool in Image Laboratory 5.0 software (Bio-Rad Laboratories). Data were presented as fold increase of normalized (to GAPDH) signal intensity of abexinostat-treated compared with DMSO-treated cells.

ChIP-Seq and ChIP-qPCR Validation

hMSC-TERT cells (vehicle or treated for 24 hours with abexinostat) pooled from three biological replicas were fixed with 1% formaldehyde for 15 minutes and quenched with 0.125 M glycine. Chromatin was isolated by the addition of lysis buffer and disruption with a Dounce homogenizer. Lysates were sonicated and the DNA sheared to an average length of 300–500 base pairs (bp). Genomic DNA (input) was prepared by treating aliquots of chromatin with RNase, proteinase K, and heat for de-crosslinking, followed by ethanol precipitation. Pellets were resuspended, and the resulting DNA was quantified on a NanoDrop spectrophotometer. Extrapolation to the original chromatin volume allowed quantitation of the total chromatin yield. An aliquot of chromatin (30 μg) was precleared with protein A agarose beads (Thermo Fisher Scientific Life Sciences). Genomic DNA regions of interest were isolated using antibodies against H3K9Ac. Complexes were washed, eluted from the beads with SDS buffer, and subjected to RNase and proteinase K treatment. Crosslinks were reversed by incubation overnight at 65°C, and ChIP DNA was purified by phenol-chloroform extraction and ethanol precipitation.

For quality assurance, qPCR reactions were carried out in triplicate on specific genomic regions using SYBR Green Supermix (Bio-Rad). The resulting signals were normalized for primer efficiency by carrying out qPCR for each primer pair using input DNA.

Illumina sequencing libraries were prepared from the ChIP and input DNAs by the standard consecutive enzymatic steps of end-polishing, dA-addition, and adaptor ligation. After a final PCR amplification step, the resulting DNA libraries were quantified and sequenced on NextSEquation 500 (75-nt reads, single end) (Illumina, San Diego, CA, http://www.illumina.com). An average of 34 million SE75 reads per sample were acquired. Reads were aligned to the human genome (hg19) using the Burrows-Wheeler alignment algorithm (default settings). Duplicate reads were removed, and only uniquely mapped reads (mapping quality $\geq$ 25) were used for further analysis. Alignments were extended in silico at their 3′ ends to a length of 200 bp, which is the average genomic fragment length in the size-selected library, and assigned to 32-nt bins along the genome. The resulting histograms (genomic "signal maps") were stored in bigWig files. Peak locations were determined by using the model-based analysis of ChIP-Seq algorithm (version 1.4.2) with a cutoff p value of 1e-7 (H3K9Ac). Signal maps and peak locations were used as input data to the Active Motif proprietary analysis program (Active Motif, Carlsbad, CA, http://www.activemotif.com), which creates Excel tables containing detailed information on sample comparisons, peak metrics, peak locations, and gene annotations. Average signal peak for each treatment condition (post-normalization) and the location of signal obtained (upstream, in gene, downstream) are listed in supplemental online Table 2. The fold change was calculated by dividing the peak signal from abexinostat-treated hMSCs to that obtained from DMSO control-treated hMSCs.

qPCR validation was subsequently conducted on an independent set of samples. An aliquot of chromatin (30 μg) was precleared with protein A agarose beads (Thermo Fisher Scientific Life Sciences). Genomic DNA regions of interest were isolated using 4 μg of antibody against H3K9Ac (catalog no. 39917; Active Motif). Complexes were washed, eluted from the beads with SDS buffer, and subjected to RNase and proteinase K treatment. Crosslinks were reversed by incubation overnight at 65°C, and ChIP DNA was purified by phenol-chloroform extraction and ethanol precipitation.

The qPCR reactions were carried out in triplicate on specific genomic regions using SYBR Green Supermix (Bio-Rad). Primer sequences used for the ChIP-qPCR experiment are listed in supplemental online Table 6. The resulting signals were normalized for primer efficiency by carrying out qPCR for each primer pair using input DNA. Data are presented as mean binding events detected per 1,000 cells. All ChIP-Seq and ChIP-qPCR experiments and data analyses were conducted by Active Motif.

Results

Epigenetic Library Screen Identified Novel Chemical Compounds That Promoted Adipocytic Differentiation of hMSCs

An epigenetic library of 24 chemical compounds was used for the initial screen. The initial screen was conducted using three

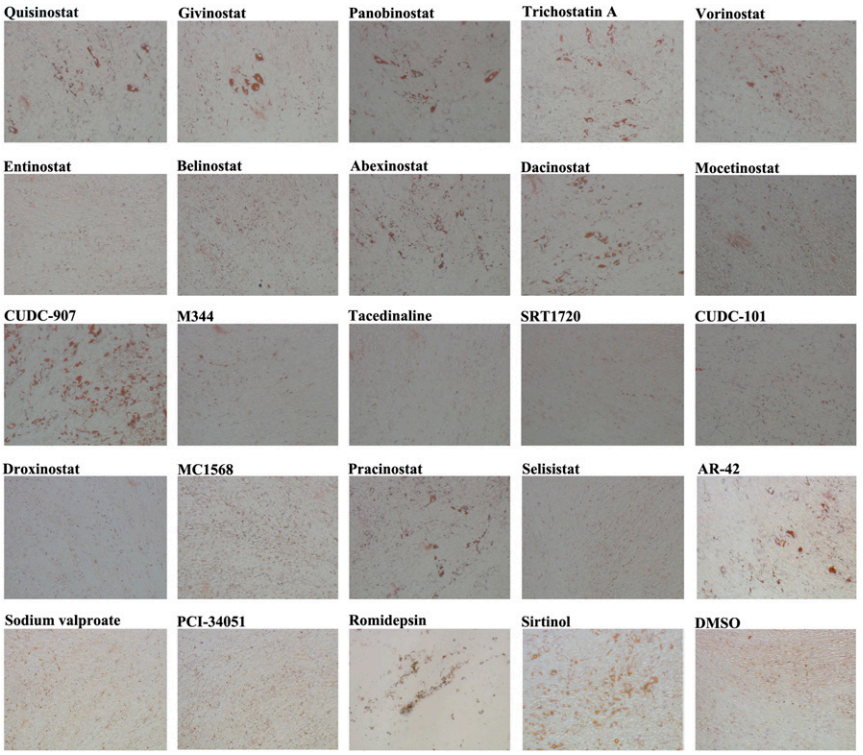

Figure 1. Epigenetic chemical compound library screen for the effect of 24 compounds on adipocytic differentiation of human skeletal (mesenchymal) stem cells (hMSCs). Representative Oil Red O staining of lipid-filled mature adipocytes on day 7 after treatment with the indicated compounds (500 nM). Images were taken at ×20 magnification using a Zeiss inverted microscope. Abbreviation: DMSO, dimethyl sulfoxide.

different doses: 20 nM, 100 nM, and 500 nM. Data presented in Figure 1 represent the 500-nM dose. Each compound was incubated with hMSCs for 24 hours at a concentration of 500 nM; cells were subsequently induced to mature adipocytes (ADs). On the basis of their ability to promote adipocyte differentiation (Fig. 1), eight compounds (abexinostat, dacinostat, CUDC-907, MC-1568, pracinostat, AR-42, PCI-34051, sirtinol) were chosen for further investigation. Gene expression analysis revealed elevated expression of *AdipoQ* in hMSCs treated with abexinostat, CUDC-907, pracinostat, and AR-42, whereas significant upregulation of *FABP4* was observed in hMSCs treated with all eight compounds compared with DMSO control (Fig. 2A).

Abexinostat Promoted Adipocytic Differentiation of hMSCs Through Induction of Several Proadipocytic Genes

We chose abexinostat for further investigation because it yielded the most consistent effects and its role in adipocyte differentiation of hMSCs has not previously been studied. We confirmed the effects of abexinostat in independent experiments. The cells were incubated for 24 hours with abexinostat (500 nM), followed by incubation in AIM for 7 days. As shown in Figure 2B, hMSCs differentiated readily into mature lipid-filled ADs, as demonstrated by positive staining for Nile Red (Fig. 2B). In addition, quantification of Nile red staining of adipocytes showed a significant increase after treatment with abexinostat ($p < .001$) (Fig. 2C).

To understand the molecular process by which abexinostat promoted adipocytic differentiation, we performed global gene expression profiling comparing abexinostat-treated and vehicle-treated control cells following adipocytic differentiation. Figure 3 illustrates hierarchical clustering based on upregulated transcripts and revealed clear separation of the abexinostat-treated and vehicle-treated control cells. We identified 1394 genes that were significantly upregulated (fold change ≥ 2.0; p (Corr) $< .05$) (supplemental online Table 1). Pathway analysis of the upregulated genes revealed strong enrichment for several cellular processes involved in adipocyte differentiation (e.g., adipogenesis, insulin-signaling, and focal adhesion). The top 10 significantly enriched pathways are illustrated in Figure 3B. The expression of selected adipocyte-related gene panel from the microarray data (*CEBPA, LPL, ACACB, NOG, LIPE, PCK1, APOC3, CNTFR, IL1RL1,* and *CXCL13*) was subsequently validated using qRT-PCR. This testing collectively corroborated the microarray data and demonstrated significant upregulation of those genes in abexinostat-treated cells, except for *ACACB*, *LIPE*, and *CXCL13*, which exhibited slight upregulation that was not, although statistically significant (Fig. 3C). Among the identified pathways, FAK and insulin signaling were more prominent given their known role in regulating adipocytic differentiation of hMSCs. Pharmacological inhibition of FAK (PF-573228) or IGF-1R/InsR (NVP-AEW51) signaling abrogated abexinostat-mediated adipocytic differentiation of hMSCs, thus implicating those pathways in this process (Fig. 3D).

Abexinostat Promoted Adipogenesis Through Inhibition of HDAC Activity

To identify the molecular mechanism by which abexinostat promotes adipocytic differentiation, hMSCs were treated with abexinostat or vehicle for 24 hours. Different histone marks were assessed using Western blotting. Data presented in Figure 4A

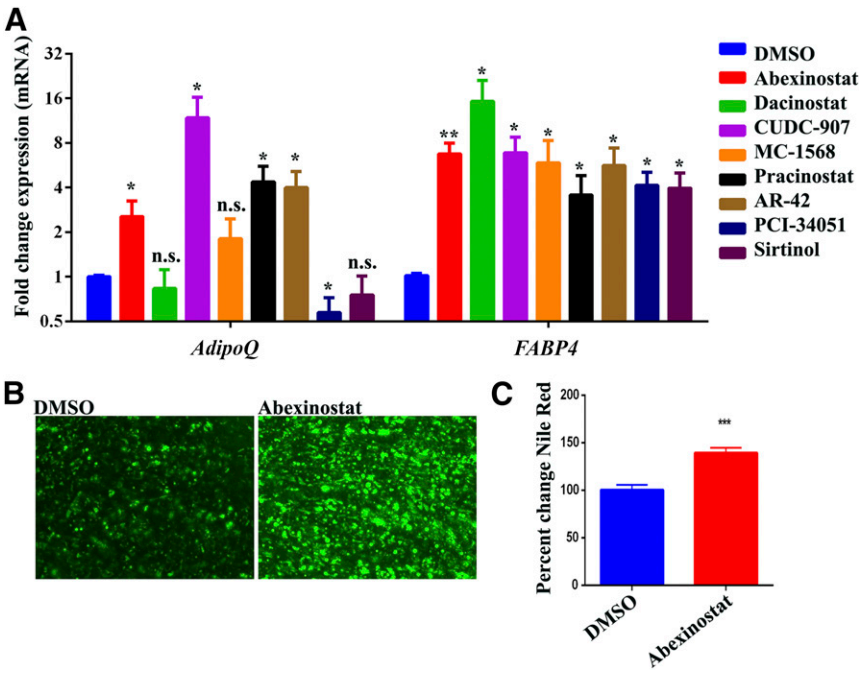

Figure 2. Effects of epigenetic chemical compounds on adipocytic differentiation of human skeletal (mesenchymal) stem cells (hMSCs). **(A):** Quantitative real-time polymerase chain reaction analysis for adipocytic marker genes (*FABP4* and *AdipoQ*) of hMSCs treated with the indicated nine chemical compounds and vehicle-treated control. Gene expression was normalized to glyceraldehyde-3-phosphate dehydrogenase. Data are presented as mean fold change ± SEM ($n = 6$) from two independent experiments. *, $p < .05$; **, $p < .005$. **(B):** Nile red staining on day 7 of postadipocytic induction of hMSCs and after exposure to abexinostat (500 nM). Images were taken at ×20 magnification using FLoid cell imaging station. **(C):** The level of Nile red staining from part **(B)** was quantified using a fluorescent microplate reader. Data are representative of three independent experiments and are presented as mean ± SEM. $n = 16$. ***, $p < .0005$. Abbreviations: DMSO, dimethyl sulfoxide; n.s., not significant.

showed increased levels of H3K9Ac, H3K4me2, and H4K8ac, all known to be associated with actively transcribed genomic regions. As expected, we observed a significant decrease in HDAC activity in abexinostat-treated cells compared with vehicle control cells ($p < .001$) (Fig. 4B). Trichostatin A-treated cells were used as positive control.

ChIP-Seq and ChIP-qPCR Data Revealed Significant Enrichment in Multiple Pathways Related to Stem Cell Differentiation

We subsequently sought to determine the genomic regions targeted by abexinostat in hMSCs. Therefore, hMSCs were treated with abexinostat for 24 hours, and subsequently we performed immunoprecipitation using an antibody against H3K9Ac, a histone mark that was markedly increased in abexinostat-treated hMSCs (Fig. 4A). The precipitated genomic DNA was then subjected to next-generation sequencing and bioinformatics analysis. Data presented in Figure 4C and 4D revealed the pull-down of a large number of genes in the abexinostat- and vehicle-treated cells. Although there were 12,105 common genes in the abexinostat- and the control-treated cells, abexinostat-treated cells revealed 306 unique genes (Fig. 4D and 4E). Supplemental online Table 2 lists all genes from the ChIP-Seq data that were enriched (1,484 genes ≥ 1.5-fold) when the abexinostat-treated cells were compared to the vehicle-treated controls. Pathway analysis performed on the genes that were significantly enriched in the abexinostat group revealed enrichment in different cellular processes related to cell differentiation, osteoblast differentiation, lipid metabolism, and Wnt pathway (Fig. 4F; supplemental online Table 3). Enrichment of H3K9Ac epigenetic mark on the promoter region of selected panel from the ChIP-Seq data or genes involved in adipogenic and osteoblastic differentiation of hMSCs (*AdipoQ, FABP4, PPARγ, KLF15, SP7, CEBPA*, and *ALPL*) was subsequently validated using ChIP-qPCR on an independent set of samples (Fig. 4G), which demonstrated a significant increase in H3K9ac signal in the promoter regions of those genes in abexinostat-treated hMSCs.

Effects of Abexinostat on Osteoblastic Differentiation of hMSCs

Interestingly, ChIP-Seq and ChIP-qPCR data revealed significant enrichment in pathways related to osteogenesis (osteoblast differentiation and Wnt receptor signaling). Therefore, we assessed the effect of abexinostat in combination with osteogenic induction medium on the osteoblastic differentiation of hMSCs. As anticipated, higher ALP staining was observed in abexinostat-treated cells compared with vehicle-treated controls (Fig. 5A). Similarly, ALP quantification performed on day 10 revealed significantly higher ALP activity in the abexinostat-treated cells compared with the control ($p < .001$) (Fig. 5B). In addition, the expression of several osteoblast-related genes (*COL1A1, SPARC, VCAM1, TGFB2, ALPL*, and *NOG*) was upregulated in abexinostat-treated cells (Fig. 5C). Concordantly, inhibition of WNT and TGFβ signaling using XAV939 or SB505124 significantly abrogated abexinostat-mediated osteogenic differentiation of hMSCs, respectively (Fig. 5D).

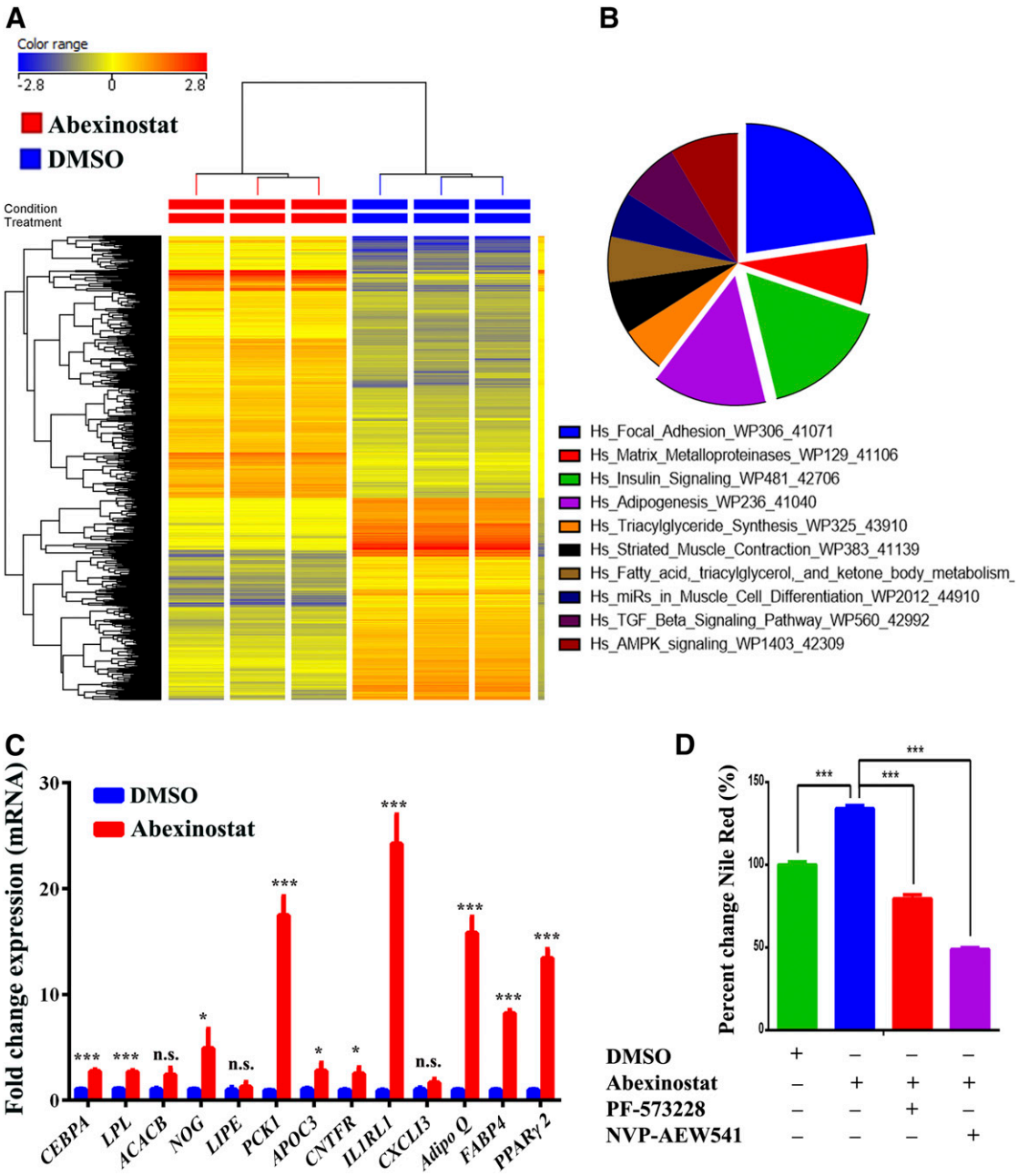

Figure 3. DNA microarray gene expression profiling of adipocyte-differentiated human skeletal (mesenchymal) stem cells (hMSCs) after abexinostat treatment. **(A):** Hierarchical clustering of abexinostat-treated versus vehicle-treated control adipocytes, based on differentially expressed mRNA transcripts. Each column represents one replica and each row represents a transcript. Expression levels of each gene in a single sample are depicted according to the color scale. **(B):** Pie chart illustrating the distribution of the top 10 enriched pathway categories in abexinostat-treated cells compared with vehicle-treated controls. **(C):** Validation of upregulated genes during adipocyte differentiation by quantitative real-time polymerase chain reaction. Gene expression was normalized to glyceraldehyde-3-phosphate dehydrogenase. Data are presented as mean fold changes ± SEM compared with DMSO controls; $n = 6$ from two independent experiments.*, $p < .05$; ***, $p < .0005$ between abexinostat-treated and DMSO-treated control cells. **(D):** Nile red quantification on day 7 after adipocytic induction of hMSCs exposed to DMSO control or abexinostat (500 nM) in the presence or absence of focal adhesion kinase (PF-573228, 5 μM) or insulin-like growth factor-1R/insulin receptor (NVP-AEW51, 5 μM) inhibitors. Data are presented as mean ± SEM; $n = 12$ from two independent experiments. ***, $p < .0005$ between each treatment condition compared with DMSO-treated control cells. Abbreviations: DMSO, dimethyl sulfoxide; n.s., not significant.

Discussion

Stem cell-based therapeutics requires development of approaches that enhance stem cell self-renewal, with the aim of obtaining a large number of cells needed for therapy and/or directing their differentiation before their clinical transplantation. Traditionally, these approaches have been achieved using hormones or growth factors/cytokines (e.g., colony-stimulating factors, erythropoietin, vitamin D or dexamethasone have been reported to enhance stem cell survival and mobilization [24]).

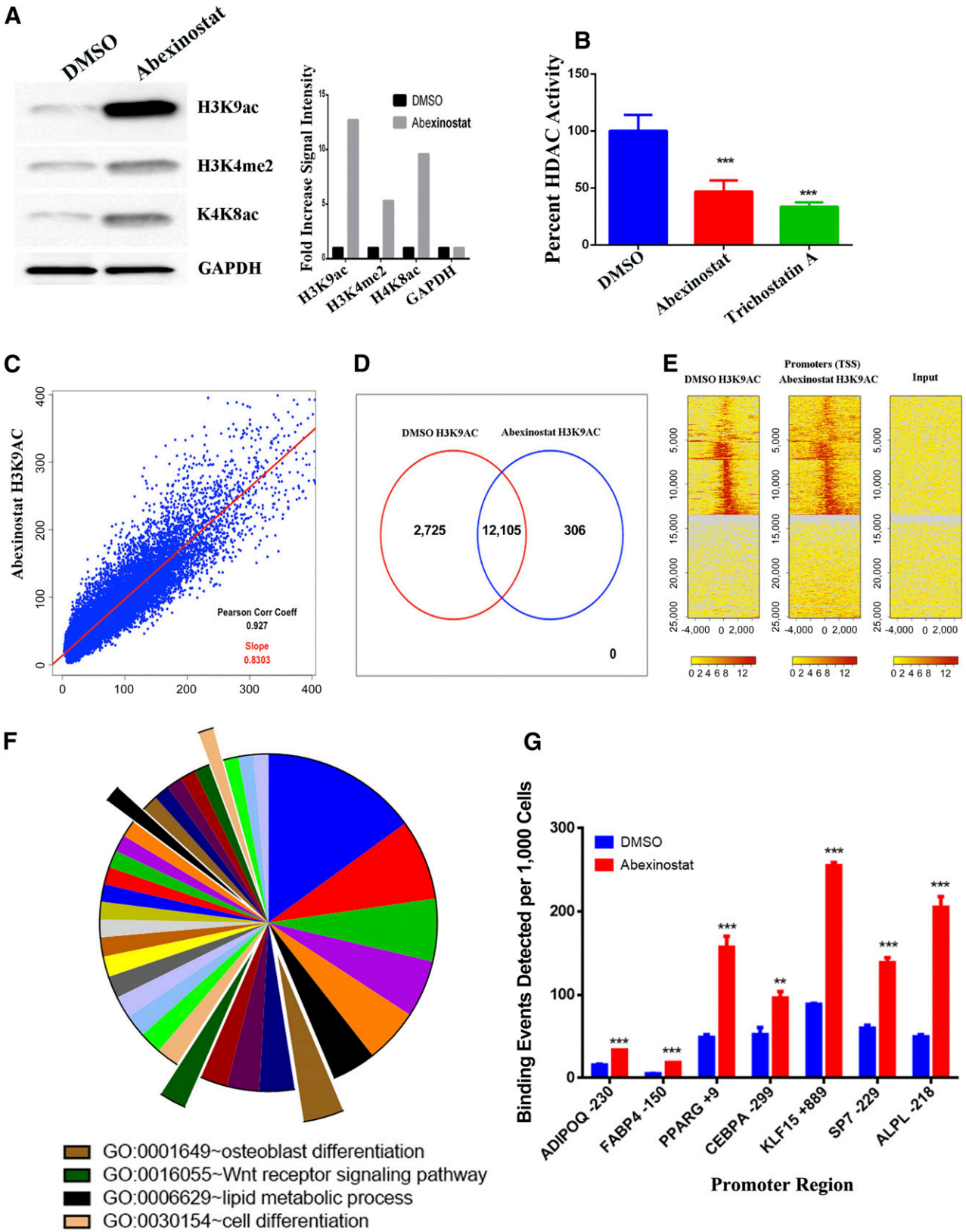

Figure 4. H3K9Ac chromatin immunoprecipitation for H3K9Ac combined with high-throughput DNA sequencing (ChIP-Seq) analysis of abexinostat-treated human skeletal (mesenchymal) stem cells (hMSCs). **(A):** Western blot analysis of histone acetylation (H3K9Ac and H4K8ac) or methylation (H3K4me2) of abexinostat-treated cells (24 hours) versus vehicle-treated controls. Data are presented as fold increase of normalized (to GAPDH) signal intensity of abexinostat- compared with DMSO-treated cells. **(B):** Quantification of total cellular histone deacetylase

(*Figure legend continues on next page*.)

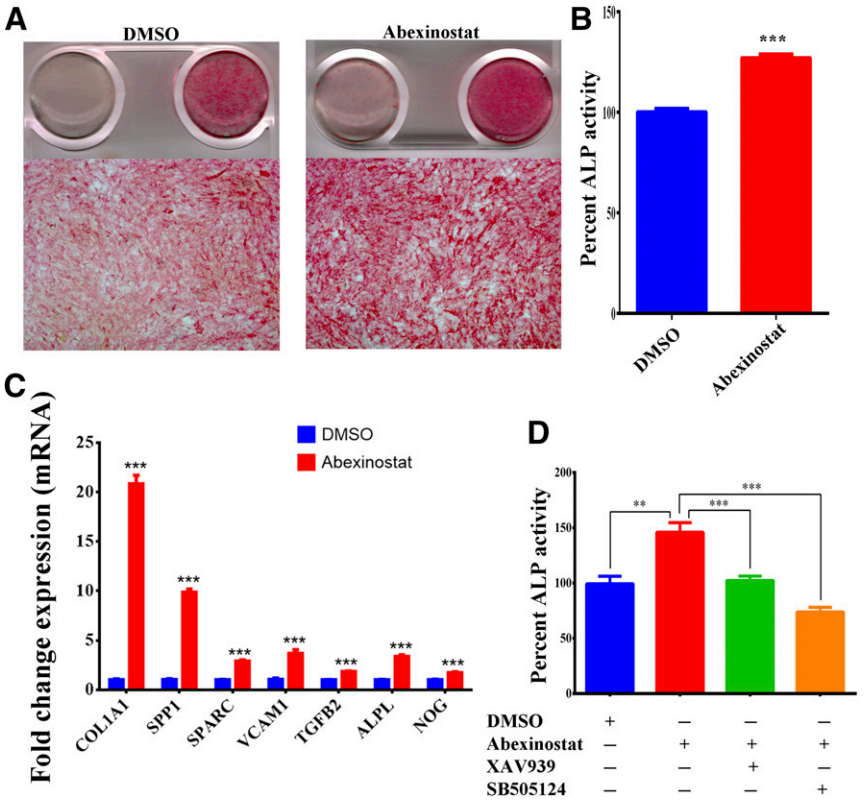

Figure 5. Effect of abexinostat treatment on osteoblastic differentiation of human skeletal (mesenchymal) stem cells (hMSCs). **(A):** ALP staining for abexinostat-treated and vehicle-treated control cells assessed on day 10 after osteoblast differentiation induction (original magnification, ×5). **(B):** Quantification of ALP activity in abexinostat-treated versus vehicle-treated control cells. Data are presented as mean ± SEM ($n = 20$). **(C):** Quantitative real-time polymerase chain reaction analysis of osteoblast-specific gene markers (*COL1A1, SPARC, VCAM1, TGFB2, ALPL*, and *NOG*). Gene expression was normalized to that of glyceraldehyde-3-phosphate dehydrogenase. Data are presented as mean ± SEM of fold change compared with control cells; $n = 9$. ***, $p < .0005$. **(D):** Quantification of ALP activity in abexinostat-treated versus vehicle-treated control cells and induced into osteoblasts (D10) in the absence or presence of WNT (XAV939) or transforming growth factor β (SB505124) inhibitors. Data are presented as mean percentage ALP activity ± SEM, $n = 20$. **, $p < .005$; ***, $p < .0005$. Abbreviations: ALP, alkaline phosphatase; DMSO, dimethyl sulfoxide.

However, using small molecule chemicals is an attractive alternative because of their ease of use, transient effects, and low cost [25, 26]. Recently, studies using epigenetic modifiers in the form of chemical compounds have been used because of their ability to alter histone acetylation/methylation or DNA methylation status, thereby regulating stem cell self-renewal or lineage-specific differentiation [27]. HDACi were successful in enhancing self-renewal of embryonic and stromal stem cells [28, 29]. We have previously reported that many microRNAs can regulate adipocyte or osteoblast differentiation of hMSCs through epigenetic-mediated mechanisms [30–32]. In the current study, we corroborated these findings because we demonstrated that the chemical compound HDACi promoted adipocytic and osteoblastic differentiation of hMSCs.

Among the initially screened compounds, we identified abexinostat, which is a novel HDACi targeting HDAC 1, 2, 3, 6, and 10 [33]. We observed that abexinostat is a potent inducer of adipogenesis, based on its ability to enhance formation of mature lipid adipocytes and enrichment of the adipocytic molecular signature of hMSCs following short-term treatment.

We observed that abexinostat induced adipocyte differentiation through upregulation of adipocyte-associated transcriptional factors known to be required for adipocyte differentiation (e.g., peroxisome proliferator-activated receptor γ [PPARγ2] and CCAAT/enhancer binding protein α [CEBPA]) [34–36]. PPARγ2 is widely accepted as an important regulator during adipogenesis, which is produced abundantly by white and brown adipocytes as

(*Figure legend continued from previous page*.)
(HDAC) enzymatic activity of abexinostat-treated hMSCs (30 minutes) compared with vehicle-treated cells. Trichostatin A (HDAC inhibitor) was used as a positive control. Data are presented as mean ± SEM ($n = 11$) from two independent experiments. ***, $p < .0005$. **(C):** Scatter plot depicting the correlation between ChIP-Seq targets identified in the vehicle-treated versus abexinostat-treated hMSCs. **(D):** Venn diagram depicting the overlap between genes identified via ChIP-Seq in the vehicle-treated controls versus abexinostat-treated hMSCs. **(E):** Promoter heat map for ChIP-Seq data in vehicle-treated versus abexinostat-treated hMSCs. Input DNA was used as reference. **(F):** Top 35 pathways for identified genes from the ChIP-Seq data that were enriched in abexinostat-treated cells compared with vehicle-treated control hMSCs (1.5-fold) presented as pie chart, wherein size of slice corresponds to fold enrichment. Selected enriched pathways are indicated. **(G):** H3K9Ac ChIP-qPCR validation for selected gene promoters regions (*AdipoQ, FABP4, PPARG, CEBPA, KLF15, SP7*, and *ALPL*) in abexinostat- vs DMSO-treated hMSCs. Data are presented as mean binding events detected per 1,000 cells ± SD; $n = 3$. Abbreviations: DMSO, dimethyl sulfoxide; GAPDH, glyceraldehyde-3-phosphate dehydrogenase.

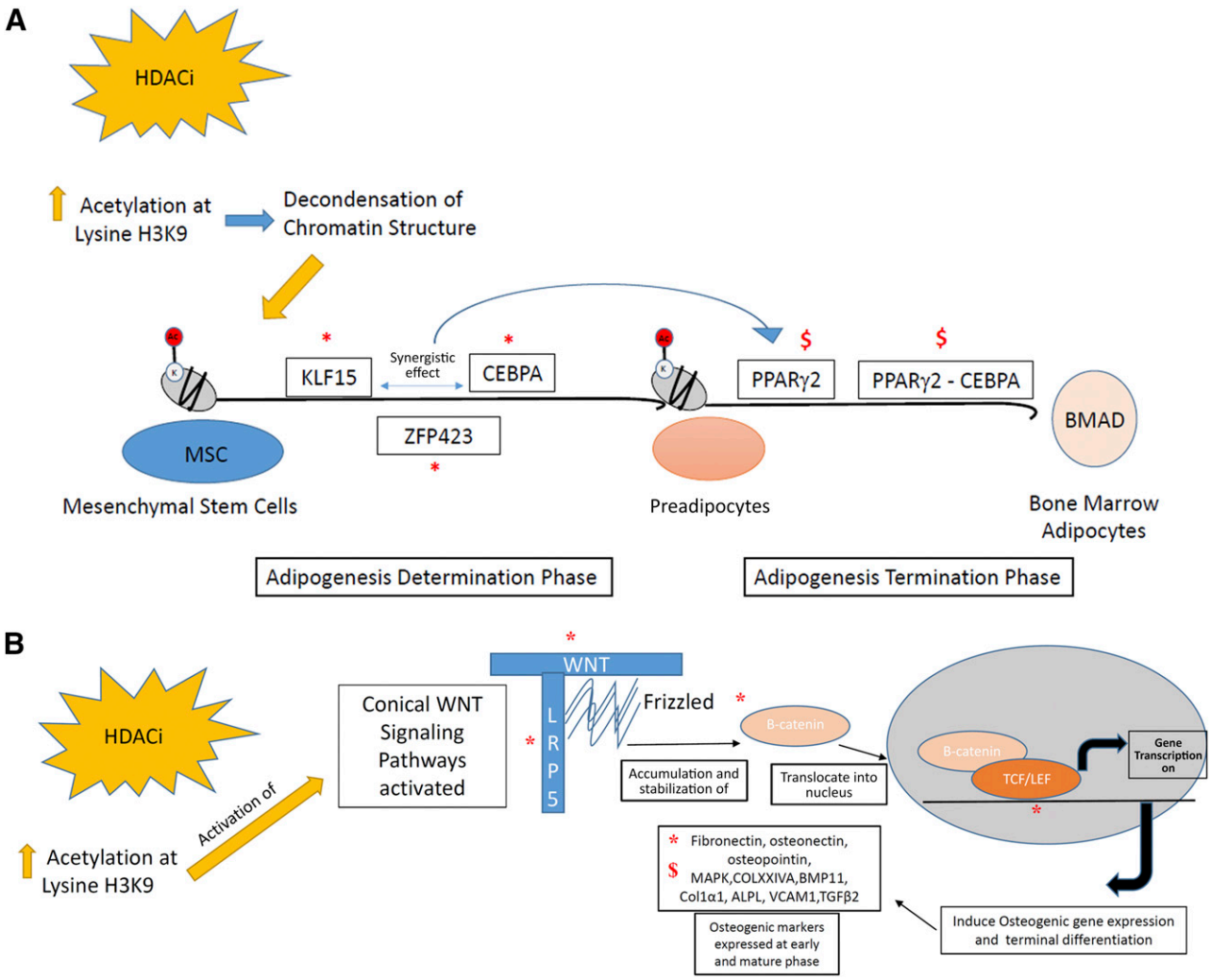

Figure 6. A working model of the molecular mechanisms of HDACi (e.g., abexinostat) on human skeletal (mesenchymal) stem cell differentiation into adipocytes and osteoblasts. **(A):** In early adipogenesis, the synergistic interaction of *KLF15* and *CEBPA* induces the expression of *PPARγ*. *PPARγ* in turn interacts with *CEBPA* to produce *FABP4* and *AdipoQ* genes involved in the expression of mature adipocyte phenotype. **(B):** HDACi-induced conical WNT signaling pathway. WNT interacts with *LRP/FZD* receptor complexes, which leads to stabilization and increases in the intracellular levels of *β*-catenin; the latter, in turn, translocates into nucleus and forms a complex with *TCF/LEF*, inducing osteogenic gene transcription (details are provided in main text). ∗, genes identified from the chromatin immunoprecipitation for H3K9Ac combined with high-throughput DNA sequencing data; $, genes identified from the gene expression microarray data. Abbreviations: BMAD, bone marrow adipocyte; HDACi, histone deacetylase inhibitors.

well as bone marrow adipocytes [35], and its expression is considered as a marker of mature bone marrow adipocytes [37].

We observed that the chromatin structure, particularly at the level of the H3 histone core of the nucleosome, exhibited a marked increase in acetylation in abexinostat-treated cells H3K9Ac. Such modifications are likely to facilitate the active state of the chromatin and to increase the accessibility of transcription factors to their target genes [35, 38–40]. In agreement with Western blotting results, ChIP-Seq data revealed dynamic alterations in histone modification after treatment with abexinostat. Among the genes identified by ChIP-seq analysis were Kruppel-like factors (KLFs), which are a family of C2H2 zinc finger proteins that regulate adipocyte differentiation [41] and induce expression of insulin-sensitive GLUT4 in muscles and adipose tissue [42]. Mori et al. [41] showed that KLF15 acts synergistically with CEBPA to induce adipogenesis via increasing the activity of PPARγ2. CEBPA and PPARγ2 act reciprocally to induce many adipogenic genes, such as *FABP4* and *AdipoQ*, that sustain their expression via a positive feedback loop and result in mature adipogenic differentiation [43]. Interestingly, ChIP-qPCR demonstrated a marked increase in H3K9ac in the promoter region of *KLF15*, *CEBPA*, and *PPARγ* in abexinostat-treated hMSCs.

Another marker that was upregulated in our ChIP-Seq data is the zinc finger protein 423, which was identified as a basic transcription factor involved in the commitment phase of adipogenic differentiation of MSCs [44]. In addition to transcriptional factors, several proteoglycans were upregulated, including chondroitin 4-sulfate glycosaminoglycan, chondroitin sulfate, and chondroitin sulfate proteoglycan. Proteoglycans exert a functional role in cell growth and cell differentiation of many cell types, including preadipocytes of 3T3-L1 cells, where they have been reported to

create a loose extracellular space between cells that will be occupied by the enlarged adipocytes during differentiation [6].

In addition to its effects on adipocyte differentiation, abexinostat enhanced osteoblast differentiation of hMSCs, and ChIP-Seq data revealed enrichment in two pathways: osteoblast differentiation and Wnt receptor signaling. Wnts are soluble lipoproteins that form a large family of secreted molecules known to play a critical role in stem/progenitor self-renewal and differentiation [45,46]. Wnts interact with receptor complexes that are formed by LRP5/LRP6 and Frizzled proteins. We observed that these Wnt receptor proteins were upregulated in our ChIP-Seq data, suggesting enhancement of Wnt signaling. The conical Wnt signaling involves the stabilization of levels of B-catenin, which in turn translocate into the nucleus and form a complex with T-cell factor (TCF)/lymphoid enhancer-binding factor, inducing target gene transcription [47]. Wnt signaling has been investigated and reviewed for its important role in MSC osteoblastic differentiation [45, 48–55]. The effect of HDACi on Wnt signaling and the activation of gene transcription of downstream genes (e.g., fibronectin, osteonectin, osteopontin, and mitogen-activated protein kinase), bone morphogenetic proteins, and members of the TGFβ superfamily may lead to enhanced osteoblastic commitment of hMSCs.

Differentiation of hMSCs into adipocytic and osteoblastic cells is usually considered to consist of two phases: the lineage commitment phase and the maturation phase. Abexinostat enhanced both osteoblast and adipocyte differentiation, and thus it is plausible that it targets the initial phase of commitment of hMSCs to both adipocytic and osteoblastic lineages. The previously mentioned and discussed data from DNA microarrays and ChIP-seq corroborate this hypothesis because they clearly demonstrate the induction of multiple gene and genetic pathways associated with hMSC lineage commitment. This hypothesis and its potential molecular mechanism are illustrated in our current working model (Fig. 6). Interestingly, despite marked global increase in H3K9Ac, we observed overall fewer enriched genes in the abexinostat-treated cells compared with the control (Fig. 4D). Therefore, it seems as if abexinostat is targeting specific genomic regions, which normally have low H3K9Ac, including those related to hMSC differentiation. On the other hand, genes with high basal H3K9ac signal are not benefiting much from abexinostat. Thus, acetylation marks appear to be being diverged from genes with high basal H3K9Ac signal (such as *GAPDH*) to those with low basal H3K9Ac signal (such as *CEBPA, PPARγ, SP7,* and *ALPL*). Nonetheless, a plausible role for abexinostat in targeting non-H3K9 residues for acetylation or the increase in hMSC commitment could also contribute to the observed phenotype.

Conclusion

Our data identified abexinostat as a novel compound promoting adipocytic and osteoblastic differentiation of hMSCs and provided new insight into the understanding of the relationship between the epigenetic effect of HDACi, transcription factors, and differentiation pathways governing adipocyte and osteoblast differentiation. Manipulating such pathways provides a novel use for epigenetic compounds in hMSC-based therapies.

Acknowledgments

We thank the College of Medicine Research Center (CMRC), Deanship for Scientific Research, King Saud University, for supporting this work.

Author Contributions

D.A: collection and/or assembly of data, data analysis and interpretation, manuscript writing; R.H.: collection and/or assembly of data; M.A. and A.A.: conception and design; M.K.: conception and design, provision of study material or patients; N.M.A.: collection and/or assembly of data, data analysis and interpretation, manuscript writing, final approval of manuscript, obtainment of funding.

Disclosure of Potential Conflicts of Interest

The authors indicated no potential conflicts of interest.

References

1 Aldahmash A, Zaher W, Al-Nbaheen M et al. Human stromal (mesenchymal) stem cells: basic biology and current clinical use for tissue regeneration. Ann Saudi Med 2012;32:68–77.

2 Abdallah BM, Jafari A, Zaher W et al. Skeletal (stromal) stem cells: An update on intracellular signaling pathways controlling osteoblast differentiation. Bone 2015;70:28–36.

3 Gan Q, Yoshida T, McDonald OG et al. Concise review: Epigenetic mechanisms contribute to pluripotency and cell lineage determination of embryonic stem cells. Stem Cells 2007;25:2–9.

4 Jenuwein T, Allis CD. Translating the histone code. Science 2001;293:1074–1080.

5 Kim SN, Choi HY, Kim YK. Regulation of adipocyte differentiation by histone deacetylase inhibitors. Arch Pharm Res 2009;32:535–541.

6 Calvo JC, Rodbard D, Katki A et al. Differentiation of 3T3-L1 preadipocytes with 3-isobutyl-1-methylxanthine and dexamethasone stimulates cell-associated and soluble chondroitin 4-sulfate proteoglycans. J Biol Chem 1991;266:11237–11244.

7 de Ruijter AJ, van Gennip AH, Caron HN et al. Histone deacetylases (HDACs): Characterization of the classical HDAC family. Biochem J 2003;370:737–749.

8 Calvanese V, Lara E, Fraga MF. Epigenetic code and self-identity. Adv Exp Med Biol 2012; 738:236–255.

9 Haberland M, Montgomery RL, Olson EN. The many roles of histone deacetylases in development and physiology: Implications for disease and therapy. Nat Rev Genet 2009; 10:32–42.

10 Xu S, De Veirman K, Evans H et al. Effect of the HDAC inhibitor vorinostat on the osteogenic differentiation of mesenchymal stem cells in vitro and bone formation in vivo. Acta Pharmacol Sin 2013;34:699–709.

11 Ververis K, Hiong A, Karagiannis TC et al. Histone deacetylase inhibitors (HDACIs): Multitargeted anticancer agents. Biologics 2013;7:47–60.

12 Minucci S, Pelicci PG. Histone deacetylase inhibitors and the promise of epigenetic (and more) treatments for cancer. Nat Rev Cancer 2006;6:38–51.

13 Falkenberg KJ, Johnstone RW. Histone deacetylases and their inhibitors in cancer, neurological diseases and immune disorders. Nat Rev Drug Discov 2014;13:673–691.

14 Paino F, La Noce M, Tirino V et al. Histone deacetylase inhibition with valproic acid downregulates osteocalcin gene expression in human dental pulp stem cells and osteoblasts: Evidence for HDAC2 involvement. Stem Cells 2014;32:279–289.

15 Dudakovic A, Evans JM, Li Y et al. Histone deacetylase inhibition promotes osteoblast maturation by altering the histone H4 epigenome and reduces Akt phosphorylation. J Biol Chem 2013;288:28783–28791.

16 Westendorf JJ, Zaidi SK, Cascino JE et al. Runx2 (Cbfa1, AML-3) interacts with histone deacetylase 6 and represses the p21(CIP1/WAF1) promoter. Mol Cell Biol 2002;22:7982–7992.

17 Schroeder TM, Nair AK, Staggs R et al. Gene profile analysis of osteoblast genes differentially regulated by histone deacetylase inhibitors. BMC Genomics 2007;8:362.

18 Schroeder TM, Westendorf JJ. Histone deacetylase inhibitors promote osteoblast maturation. J Bone Miner Res 2005;20:2254–2263.

19 Yoo EJ, Chung JJ, Choe SS et al. Down-regulation of histone deacetylases stimulates

adipocyte differentiation. J Biol Chem 2006; 281:6608–6615.

20 Kuzmochka C, Abdou HS, Haché RJ et al. Inactivation of histone deacetylase 1 (HDAC1) but not HDAC2 is required for the glucocorticoid-dependent CCAAT/enhancer-binding protein α (C/EBPα) expression and preadipocyte differentiation. Endocrinology 2014;155:4762–4773.

21 Zhou Y, Peng J, Jiang S. Role of histone acetyltransferases and histone deacetylases in adipocyte differentiation and adipogenesis. Eur J Cell Biol 2014;93:170–177.

22 Abdallah BM, Haack-Sørensen M, Burns JS et al. Maintenance of differentiation potential of human bone marrow mesenchymal stem cells immortalized by human telomerase reverse transcriptase gene despite [corrected] extensive proliferation. Biochem Biophys Res Commun 2005;326:527–538.

23 Livak KJ, Schmittgen TD. Analysis of relative gene expression data using real-time quantitative PCR and the 2(-Delta Delta C(T)) Method. Methods 2001;25:402–408.

24 Romagnani P, Lasagni L, Mazzinghi B et al. Pharmacological modulation of stem cell function. Curr Med Chem 2007;14:1129–1139.

25 Ding S, Schultz PG. A role for chemistry in stem cell biology. Nat Biotechnol 2004;22:833–840.

26 Lu B, Atala A. Small molecules and small molecule drugs in regenerative medicine. Drug Discov Today 2014;19:801–808.

27 Romanov YA, Darevskaya AN, Merzlikina NV et al. Mesenchymal stem cells from human bone marrow and adipose tissue: isolation, characterization, and differentiation potentialities. Bull Exp Biol Med 2005;140:138–143.

28 Lee JH, Kim KA, Kwon KB et al. Diallyl disulfide accelerates adipogenesis in 3T3-L1 cells. Int J Mol Med 2007;20:59–64.

29 Jamaladdin S, Kelly RD, O'Regan L et al. Histone deacetylase (HDAC) 1 and 2 are essential for accurate cell division and the pluripotency of embryonic stem cells. Proc Natl Acad Sci USA 2014;111:9840–9845.

30 Hamam D, Ali D, Kassem M et al. microRNAs as regulators of adipogenic differentiation of mesenchymal stem cells. Stem Cells Dev 2015;24:417–425.

31 Hamam D, Ali D, Vishnubalaji R et al. microRNA-320/RUNX2 axis regulates adipocytic differentiation of human mesenchymal (skeletal) stem cells. Cell Death Dis 2014;5:e1499.

32 Eskildsen T, Taipaleenmäki H, Stenvang J et al. MicroRNA-138 regulates osteogenic differentiation of human stromal (mesenchymal) stem cells in vivo. Proc Natl Acad Sci USA 2011;108:6139–6144.

33 Buggy JJ, Cao ZA, Bass KE et al. CRA-024781: A novel synthetic inhibitor of histone deacetylase enzymes with antitumor activity in vitro and in vivo. Mol Cancer Ther 2006;5: 1309–1317.

34 Rosen ED, Walkey CJ, Puigserver P et al. Transcriptional regulation of adipogenesis. Genes Dev 2000;14:1293–1307.

35 Christodoulides C, Lagathu C, Sethi JK et al. Adipogenesis and WNT signalling. Trends Endocrinol Metab 2009;20:16–24.

36 Ali AT, Hochfeld WE, Myburgh R et al. Adipocyte and adipogenesis. Eur J Cell Biol 2013; 92:229–236.

37 Krings A, Rahman S, Huang S et al. Bone marrow fat has brown adipose tissue characteristics, which are attenuated with aging and diabetes. Bone 2012;50:546–552.

38 Cristancho AG, Lazar MA. Forming functional fat: A growing understanding of adipocyte differentiation. Nat Rev Mol Cell Biol 2011;12:722–734.

39 Moreno-Navarret JM, Fernández-Real JM. Adipocyte differentiation. In: Symonds MEE, ed. Adipose Tissue Biology. New York, NY: Springer Science+Business Media, 2012:17–38.

40 Duncan HF, Smith AJ, Fleming GJ et al. Epigenetic modulation of dental pulp stem cells: Implications for regenerative endodontics. Int Endod J 2016;49:431–446.

41 Mori T, Sakaue H, Iguchi H et al. Role of Krüppel-like factor 15 (KLF15) in transcriptional regulation of adipogenesis. J Biol Chem 2005; 280:12867–12875.

42 Gray S, Feinberg MW, Hull S et al. The Krüppel-like factor KLF15 regulates the insulin-sensitive glucose transporter GLUT4. J Biol Chem 2002;277:34322–34328.

43 Scotti E, Tontonoz P. Peroxisome proliferator-activated receptor gamma dances with different partners in macrophage and adipocytes. Mol Cell Biol 2010;30:2076–2077.

44 Wei S, Zhang L, Zhou X et al. Emerging roles of zinc finger proteins in regulating adipogenesis. Cell Mol Life Sci 2013;70:4569–4584.

45 Liu G, Vijayakumar S, Grumolato L et al. Canonical Wnts function as potent regulators of osteogenesis by human mesenchymal stem cells. J Cell Biol 2009;185:67–75.

46 Mo S, Cui Z. Regulation of canonical Wnt signaling during development and diseases. In: Sato K, ed. Embryogenesis. Rijeka, Croatia: InTech, 2012:67–110.

47 Arvidson K, Abdallah BM, Applegate LA et al. Bone regeneration and stem cells. J Cell Mol Med 2011;15:718–746.

48 Qiu W, Hu Y, Andersen TE et al. Tumor necrosis factor receptor superfamily member 19 (TNFRSF19) regulates differentiation fate of human mesenchymal (stromal) stem cells through canonical Wnt signaling and C/EBP. J Biol Chem 2010;285:14438–14449.

49 Qiu W, Andersen TE, Bollerslev J et al. Patients with high bone mass phenotype exhibit enhanced osteoblast differentiation and inhibition of adipogenesis of human mesenchymal stem cells. J Bone Miner Res 2007;22:1720–1731.

50 Boland GM, Perkins G, Hall DJ et al. Wnt 3a promotes proliferation and suppresses osteogenic differentiation of adult human mesenchymal stem cells. J Cell Biochem 2004;93: 1210–1230.

51 Gaur T, Lengner CJ, Hovhannisyan H et al. Canonical WNT signaling promotes osteogenesis by directly stimulating Runx2 gene expression. J Biol Chem 2005;280:33132–33140.

52 Glass DA 2nd, Bialek P, Ahn JD et al. Canonical Wnt signaling in differentiated osteoblasts controls osteoclast differentiation. Dev Cell 2005;8:751–764.

53 Ling L, Nurcombe V, Cool SM. Wnt signaling controls the fate of mesenchymal stem cells. Gene 2009;433:1–7.

54 Liu F, Kohlmeier S, Wang CY. Wnt signaling and skeletal development. Cell Signal 2008; 20:999–1009.

55 Piters E, Boudin E, Van Hul W. Wnt signaling: a win for bone. Arch Biochem Biophys 2008; 473:112–116.

See www.StemCellsTM.com for supporting information available online.

